Journal of Dentistry 80 (2019) 15–22

Contents lists available at ScienceDirect

Journal of Dentistry

journal homepage: www.elsevier.com/locate/jdent

Nanocomplexes of carboxymethyl chitosan/amorphous calcium phosphate reduce oral bacteria adherence and biofilm formation on human enamel surface☆

Jiankang He[a], Yijun Bao[a], Jie Li[a], Zhongjun Qiu[b], Ying Liu[a,*], Xu Zhang[a,**]

[a] School of Stomatology, Hospital of Stomatology, Tianjin Medical University, 12 Observatory Road, Tianjin, 300070, China
[b] State Key Laboratory of Precision Measuring Technology & Instruments, Tianjin University, Tianjin, 300072, China

ARTICLE INFO

Keywords:
Nanocomplexes
Carboxymethyl chitosan/amorphous calcium phosphate
Oral bacteria
Enamel
Microbial adherence
Biofilm formation

ABSTRACT

Objectives: This study investigated the effect of CMC/ACP on oral bacteria adherence and biofilm formation on the enamel surface as well as the underlying mechanism to determine the anti-cariogenic potential of CMC/ACP.

Methods: A mineral solution of CMC/ACP was characterised by transmission electron microscope. The bactericidal activity of CMC/ACP was evaluated with the plate count method. An *in vitro* biofilm model was established on saliva-coated enamel blocks; the effect of CMC/ACP on the adherence of *Streptococcus mutans* and *Streptococcus gordonii* to and biofilm formation on these blocks, as well as co-aggregation of *Fusobacterium nucleatum* was assessed by scanning electron microscopy, crystal violet staining, and confocal microscopy. Bacterial surface charge was estimated with the cytochrome c binding assay and by zeta potential measurement.

Results: CMC/ACP nanocomplexes inhibited *S. mutans* and *S. gordonii* adherence to enamel blocks by 90% and 86% ($P < 0.01$), respectively, and biofilm formation by 45% and 44% ($P < 0.01$), respectively, after 24 h without bactericidal activity. CMC/ACP reduced *F. nucleatum* attachment to streptococcal biofilm by 75% ($P < 0.01$) while also altering cytochrome c binding to bacteria and reducing the zeta potential of the bacterial suspension.

Conclusions: CMC/ACP nanocomplexes inhibit cariogenic bacterial adherence, co-adhesion, and biofilm formation on the enamel surface, possibly by altering bacterial surface charge and enhancing the flocculation effect. As an agent that promotes remineralisation and has anti-cariogenic effects, CMC/ACP can be used to prevent and treat early caries and white spot lesions.

1. Introduction

Dental caries is one of the most prevalent and costly diseases worldwide and can have a profound effect on general health and quality of life [1]. With the increasing popularity of orthodontic treatments, the incidence of enamel surface white spot lesions (WSLs) caused by orthodontic appliances has shown an upward trend [2,3]. WSLs are a type of early smooth surface caries characterised by the demineralisation of the enamel surface around orthodontic appliances [4,5]. Demineralisation is a pathological process caused by organic acids produced by dental plaque biofilms formed on the enamel surface; cariogenic bacteria within the biofilms release acid, which lowers the local pH and results in the loss of calcium and phosphate ions from the hydroxyapatite lattice of enamel [6,7]. Dental caries and WSL formation are dynamic processes associated with an imbalance between demineralisation and remineralisation [8]. As such, one approach for halting their progression is to treat early lesions with a remineralising agent. This is not only consistent with the concept of minimally invasive dentistry (MID) [9], but also benefits patients by reducing trauma and treatment costs and preserving natural dental tissue.

Nanoparticles of amorphous calcium phosphate (ACP) stabilised by biomacromolecules can be used for enamel remineralisation [10,11]. However, multiple species of bacteria colonise the oral environment; bacterial biofilms tend to aggregate on rough surfaces and cariogenic

☆ Clinical significance: This study demonstrates that in addition to their remineralisation function, carboxymethyl chitosan/amorphous calcium phosphate nanocomplexes inhibit the adherence of and biofilm formation by cariogenic bacteria including *Streptococcus mutans* and *Streptococcus gordonii* on the enamel surface. Thus, this biomaterial can potentially be used to treat early caries and white spot lesions.

* Corresponding author at: Department of Endodontics, Hospital of Stomatology, Tianjin Medical University, 12 Observatory Road, Tianjin, 300070, China.
** Corresponding author.
E-mail addresses: yingliu04@tmu.edu.cn (Y. Liu), zhangxu@tmu.edu.cn, zhxden@gmail.com (X. Zhang).

https://doi.org/10.1016/j.jdent.2018.11.003
Received 4 September 2018; Received in revised form 26 October 2018; Accepted 6 November 2018

bacteria in biofilms continually produce acid. The colonisation of oral bacteria cannot be inhibited by biomimetic remineralisation agents such as casein phosphopeptide/ACP [12,13]. Therefore, while promoting the deposition of calcium and phosphorus on carious lesions, remineralisation agents may also promote the mineralization of plaques to form a harder and often tenacious mass called calculus, which may increase the risk of plaque-related diseases [14,15].

The first step in biofilm formation is the adherence of bacteria to the acquired pellicle on the enamel surface [16,17]. *Streptococcus* is the predominant genus detected on salivary pellicles [18–20], and *Streptococcus mutans* is the primary causative bacterial agent of dental caries [21,22]. *Streptococcus gordonii* is a pioneer coloniser of tooth surfaces and produces multiple cell surface protein adhesins that promote attachment to the salivary pellicle and provide a foundation for the formation of mixed-species dental plaque biofilms [23,24]. Additionally, some species such as *Fusobacterium nucleatum* play a critical role as a so-called bridge species in biofilm development by selectively co-aggregating with early and late colonisers [25–27]. Thus, strategies that promote remineralisation while inhibiting biofilm formation on enamel surfaces are needed for clinical dentistry.

Our previous study showed that carboxymethyl chitosan (CMC)—a derivative of chitosan that is biodegradable, biocompatible, and non-toxic—is an excellent stabiliser of ACP nanoparticles owing to its abundance of carboxyl groups; CMC/ACP nanocomplexes were effective in promoting the remineralisation of dental tissues [28,29]. Other studies have shown that CMC can inhibit biofilm formation of some pathogenic bacteria such as *Escherichia coli* and *Staphylococcus aureus* [30,31]. However, it is unclear how ACP influences the inhibitory effect of CMC on oral bacterial biofilm formation.

An *in vitro* model of cariogenic bacterial biofilm on the human enamel surface that mimics the oral environment has been established [32]. In the present study, we used this model to investigate the effects of CMC/ACP on the adherence of and biofilm formation by cariogenic bacterial species on enamel, the co-adhesion of *F. nucleatum*, and the underlying mechanism. We hypothesised that CMC/ACP nanocomplexes can inhibit these processes and thereby promote oral health.

2. Materials and methods

2.1. Bacterial culture

S. mutans UA159 and *Streptococcus gordonii* ATCC10558 were cultured in brain-heart infusion (BHI) medium (Sigma-Aldrich, St. Louis, MO, USA) under anaerobic conditions (10% CO_2, 10% H_2, and 80% N_2). *F. nucleatum* ATCC25586 was cultured anaerobically in BHI medium supplemented with haemin (10 mg/ml) and vitamin K (0.2 mg/ml). All cultures were grown at 37 °C.

2.2. Enamel blocks and hydroxyapatite discs

Four hundred and eighty-six enamel blocks ($\sim 4 \times 3 \times 2$ mm^3 in size) removed by sawing from the buccal or lingual surfaces of freshly extracted 120 human third molars and polished with 400- to 2000-grit SiC paper were used as the substratum. The molars were obtained from patients aged 18–30 years who required preventive extraction before orthodontic therapy at the Hospital of Stomatology. The inclusion criterion was that the tooth enamel was mature and lacked caries, cracks, or other defects. Hydroxyapatite discs (n = 162) (5.0 mm in diameter and 2.0 mm in thickness) were used as a substratum for confocal scanning laser microscopy analysis. All enamel blocks and hydroxyapatite discs were autoclaved and stored in sterile tubes. The study was approved by the ethics committee (TMUSHhMEC2017090).

2.3. Preparation of CMC/ACP mineral solution

A 1% (m/v) CMC/ACP mineral solution with biomimetic remineralisation function was prepared as previously described [33]. Briefly, the CMC solution was first prepared by mixing 400 mg CMC powder (95%; Qingdao Hong Hai Biological Technology Co., Qingdao, China) with 30 ml deionised water and stirring (1000 rpm) until the powder was completely dissolved. Next, 41.76 mg K_2HPO_4 were added to the CMC solution with gentle stirring (500 rpm). $CaCl_2{\cdot}2H_2O$ (58.80 mg) was then added to 10 ml deionised water, and the mixture was introduced into the CMC solution with stirring (500 rpm) for 5 min, yielding a highly supersaturated CMC/ACP mineral solution. The final concentrations of calcium and phosphate ions were 10 and 6 mM, respectively.

2.4. Characterisation of CMC/ACP nanocomplexes

The size and morphology of nanocomplexes formed by CMC/ACP nanoparticles were characterised by transmission electron microscopy (TEM) (JEM-1230; JEOL, Tokyo, Japan) and selected area electron diffraction (SAED) at 110 kV. A 15-ml volume of nanoparticle solution was added as a drop onto a 400-mesh copper TEM grid covered with a carbon support film at room temperature.

2.5. Preparation of salivary pellicle

Non-stimulated whole saliva samples were collected from 10 healthy adult volunteers as previously described [34], and mixed and immediately centrifuged at 12,000 × *g* for 20 min at 4 °C. After sterile filtration, enamel blocks were treated with saliva for 30 min at 37 °C to obtain salivary pellicle.

2.6. Antibacterial test

The antibacterial activity of CMC/ACP was evaluated with the plate count method [35,36]. Briefly, *S. mutans*, *S. gordonii*, and *F. nucleatum* were harvested by centrifugation at 5000 rpm for 5 min, washed with phosphate-buffered saline (PBS), and resuspended in BHI medium; the optical density at 600 nm (OD_{600}) was adjusted to 0.8 (approximately 1×10^8 CFU/ml), and the cell suspension was diluted with an equivalent volume of CMC/ACP, CMC, or deionised water, and incubated for 24 h at 37 °C under anaerobic conditions; the final concentration of CMC/ACP and CMC was 0.5% (m/v). A 200-μl volume of bacterial suspension was serially diluted and 100 μl was spread on a 2% agar plate in triplicate and incubated for 24 h at 37 °C under anaerobic conditions, after which the number of viable colonies was counted. The experiment was repeated three times for each strain.

2.7. Bacterial adhesion assay

For the microbial adherence assay [37], *S. mutans* or *S. gordonii* was harvested and resuspended as described above to a density of 10^7 CFU/ml. A 200-μl volume of streptococcal suspension was combined with an equal volume of CMC/ACP, CMC, or deionised water, and the mixture was added to the enamel blocks (n = 9) in a 48-well plate, followed by incubation at 37 °C for 1 or 5 h; the final concentration of CMC/ACP and CMC was 0.5% (m/v). To quantify the bacteria adhering to the enamel blocks, samples were fixed in 2.5% glutaraldehyde solution, rinsed with distilled water, and dehydrated in a graded series of ethanol solution (50%, 60%, 70%, 80%, 90%, and 100%) for 15 min. Samples were then dried to the critical point, coated with gold, and examined by scanning electron microscopy (SEM) (JSM-6701 F; JEOL). Adherent cells in nine randomly selected 3000-fold magnification fields were counted, and the number of bacteria in 1 mm^2 was calculated.

2.8. Biofilm formation assay

For the biofilm formation assay, streptococcal suspension was diluted to 2×10^6 CFU/ml with BHI medium supplemented with 1%

sucrose. A 200-μl volume of suspension was added to a 48-well plate with saliva-coated enamel blocks (n = 9) along with an equal volume of CMC/ACP, CMC, or deionised water, followed by incubation at 37 °C for 24 h under anaerobic conditions; the final concentration of CMC/ACP and CMC was 0.5% (m/v). After incubation, the enamel blocks were rinsed three times with PBS, and biofilm formed on the block surface was stained with 0.1% (w/v) crystal violet for 15 min, washed three times with PBS, and destained with 400 μl of 80% (v/v) ethanol solution. To determine the amount of bacteria in the formed biofilms, the absorbance at 590 nm of the destaining solution containing crystal violet was measured using a microplate reader (Synergy Mx; BioTek, Winooski, VT, USA) as previously described [38].

2.9. Attachment of F. nucleatum to streptococcal biofilm

The effect of CMC/ACP on *F. nucleatum* attachment to the streptococcal biofilm was evaluated by fluorescence staining [39–41]. *S. mutans* and *S. gordonii* cultures (10 ml) were harvested by centrifugation at 5000 rpm and resuspended in 1 ml PBS. Cells were labelled with 20 μl of 10 mM hexidium iodide (Thermo Fisher Scientific, Waltham, MA, USA) for 15 min in the dark, centrifuged at 5000 rpm for 5 min, and washed with PBS. For all experiments, the OD_{600} of the cell suspension was adjusted to 0.8, and a 400-μl aliquot was added to each well of a 48-well plate containing a saliva-coated hydroxyapatite disc (n = 9) followed by incubation at 37 °C for 24 h under anaerobic conditions in the dark. The discs were then carefully rinsed with PBS and coated with saliva. Similarly, *F. nucleatum* cultures (10 ml) were harvested as described above, labelled with 20 μl of 4 mg/ml carboxyfluorescein diacetate succinimidyl ester (CFSE) (Thermo Fisher Scientific) for 15 min in dark; after washing three times with PBS, 200 μl CFSE-labelled *F. nucleatum* suspension (OD_{600} = 1) was added to the saliva-coated hydroxyapatite disc along with an equal volume of CMC/ACP, CMC, or deionised water; the final concentration of CMC/ACP and CMC was 0.5% (m/v). The samples were then incubated for 24 h at 37 °C under anaerobic conditions in the dark. The supernatant was removed, and the cells were washed with PBS to remove those that were non-adherent or loosely bound. The attachment of *F. nucleatum* to streptococcal biofilms was visualised by confocal laser scanning microscopy (Axio-Imager LSM-800; Carl Zeiss, Oberkochen, Germany). For each sample, images were obtained from five randomly selected areas at 400-fold magnification and were analysed with Imaris v.7.2.3 image analysis software (Bitplane, Concord, MA, USA) to determine the ratio of green to red fluorescence (GR ratio).

2.10. Bacteria cell surface charge assay

The cytochrome c binding assay was used to estimate bacterial surface charge [30]. *S. mutans* or *S. gordonii* was harvested and resuspended as described above to a density of 10^8 CFU/ml; the cell suspension was then mixed with an equal volume of CMC/ACP, CMC, or deionised water and cultured for 1 h at 37 °C under anaerobic conditions; the final concentration of CMC/ACP and CMC was 0.5% (m/v). The cells were harvested by centrifugation, rinsed, and resuspended in (3-(*N*-morpholino)propanesulfonic acid) buffer (pH 7.0) to a final OD_{600} of 7.0. After incubation with 0.5 mg/ml cytochrome c for 10 min, the cells were removed by centrifugation at 12,000 rpm for 5 min at 4 °C. The amount of cytochrome c in the supernatant was quantified by measuring the OD at 530 nm with a microplate reader. The percent change in cytochrome c bound to the cells was calculated as follows: $\left(1 - \frac{\text{ODsample}}{\text{ODcontrol}}\right) \times 100\%$.

The zeta potential values of CMC, CMC/ACP, and each experimental group was estimated as previously described [42–44]. Briefly, *S. mutans* cells were concentrated by centrifugation at 5000 rpm and resuspended in PBS to an OD_{600} of 1.0. CMC/ACP, CMC, or PBS was added to the cells and after 1 h, the zeta potential was measured using a Zetasizer Nano ZS 90 device (Malvern Instruments, Malvern, UK) at room temperature.

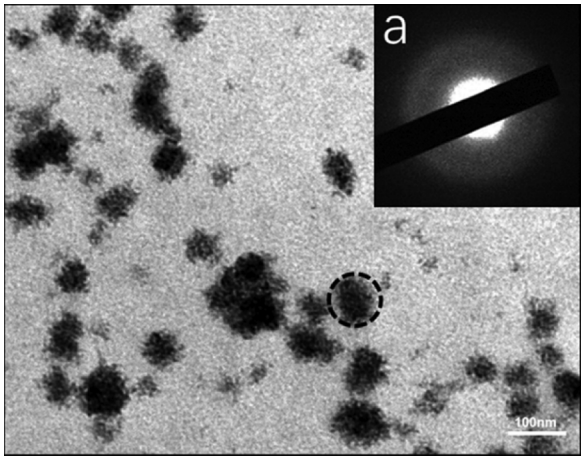

Fig. 1. TEM and SAED characterisation of nanocomplexes of CMC/ACP. The image of TEM show the shape and morphology of nanocomplexes of CMC/ACP. The inset(a)in Fig. 1 : The SAED of nanoparticles of CMC/ACP show there is no obvious dot or ring pattern characteristic of crystal structure.

2.11. Statistical analysis

Statistical analysis was performed with SPSS v.22.0 software (IBM, Armonk, NY, USA). Differences between groups were evaluated by one-way analysis of variance with the Tukey-Kramer multiple comparisons post-hoc test and with the two-tailed unpaired *t*-test $P < 0.05$ was considered statistically significant.

3. Results

3.1. Examination of CMC/ACP nanoparticle morphology by TEM and SAED

The size and morphology of CMC/ACP nanoparticles were evaluated by TEM (Fig. 1). The particles had a diameter < 100 nm and had a rough surface. SAED analysis did not reveal an obvious dot or ring pattern characteristic of crystal structures (inset a in Fig. 1), indicating that the CMC/ACP nanoparticles mainly constituted an amorphous phase.

3.2. Bactericidal activity

The bactericidal and bacteriostatic activities of CMC/ACP were examined by the plate count method. After culturing for 24 h, there were no significant differences among groups in terms of the number of live colonies on the agar plates. These results suggest that CMC and CMC/ACP do not interfere with the growth and viability of *S. mutans*, *S. gordonii*, and *F. nucleatum* at a concentration of 1% (Table 1).

3.3. Effect of CMC/ACP on S. mutans and S. gordonii adherence to saliva-coated enamel blocks

The effect of CMC/ACP on *S. mutans* and *S. gordonii* adherence to saliva-coated enamel blocks was evaluated by SEM. The adherence of *S. mutans* and *S. gordonii* to saliva-coated enamel blocks was inhibited in the presence of CMC/ACP by 89.7% and 86.1% ($P < 0.01$), respectively, at 1 h (Fig. 2A, C) and by 80.8% and 82.1% ($P < 0.01$), respectively, at 5 h (Fig. 2B, D). There was no significant difference between CMC/ACP and CMC groups.

Table 1
Colony counts of viable colonies after 24 h-incubation on agar plates. The bactericidal and bacteriostatic activities of CMC/ACP were examined by the plate count method. CFU on the agar plates were counted and expressed as the means ± SD, the experiments were performed three times in triplicate, $^{\#}$P = not significant compared with the control value (absence of CMC/ACP or CMC). CFU, colony-forming unit.

Bacterial strains	CFU		
	Control	CMC	CMC/ACP
S. mutans	$(1.60 \pm 0.12) \times 10^8$	$(1.58 \pm 0.23) \times 10^{8\#}$	$(1.59 \pm 0.12) \times 10^{8\#}$
S. gordonii	$(5.50 \pm 0.10) \times 10^7$	$(5.53 \pm 0.13) \times 10^{7\#}$	$(5.63 \pm 0.18) \times 10^{7\#}$
F. nucleatum	$(1.70 \pm 0.11) \times 10^8$	$(1.65 \pm 0.21) \times 10^{8\#}$	$(1.63 \pm 0.23) \times 10^{8\#}$

3.4. Effect of CMC/ACP on S. mutans and S. gordonii biofilm formation on saliva-coated enamel blocks

The effect of CMC/ACP on *S. mutans* and *S. gordonii* biofilm formation on saliva-coated enamel blocks was evaluated by crystal violet staining. Biofilm formation (control = 100%) was decreased by 45.3% (*S. mutans*) and 44.0% (*S. gordonii*) after incubation for 24 h with CMC/ACP ($P < 0.01$; Fig. 3). There was no significant difference between the CMC/ACP and CMC groups (Fig. 3).

3.5. Effect of CMC/ACP on F. nucleatum attachment to pre-formed streptococcal biofilm on saliva-coated hydroxyapatite disc

The effect of CMC/ACP on the attachment of *F. nucleatum* to saliva-coated streptococcal biofilm was evaluated by fluorescence staining. The biofilm formed on saliva-coated hydroxyapatite discs was stained with hexidium iodide, and CFSE-labelled *F. nucleatum* was then added in the presence or absence of CMC/ACP. *F. nucleatum* attachment to the biofilm was quantified by determining the GR ratio. In the absence of CMC/ACP, a large number of *F. nucleatum* (green fluorescent signal) adhered to the *Streptococcus* biofilm (red fluorescent signal) after 24 h of co-culture (Fig. 4A). Addition of CMC/ACP decreased the number of *F. nucleatum* cells bound to the pre-formed *S. mutans* or *S. gordonii* biofilm. Accordingly, the GR ratio was decreased by 74.6% and 74.9%, respectively, in the presence of CMC/ACP ($P < 0.01$; Fig. 4B). There was no significant difference between CMC/ACP and CMC groups in terms of *F. nucleatum* attachment.

3.6. Effect of CMC/ACP on cell surface charge

Cytochrome c and zeta potential were measured in order to estimate the relative charge of the cell surface. CMC/ACP reduced cytochrome c binding to *S. mutans* and *S. gordonii* cells by 12.6% and 11.9%, respectively ($P < 0.01$; Fig. 5), indicating that their surface charge was altered. The average zeta potential of CMC, CMC/ACP, and untreated *S. mutans* was −41.6, −28.1, and −38.2 mV, respectively; however, 1 h after adding CMC or CMC/ACP, the zeta potential of *S. mutans* decreased to −31.3 and −22.1 mV, respectively, which was significantly lower than the value of untreated *S. mutans* suspension ($P < 0.05$; Fig. 6), and the zeta potential of the CMC/ACP groups was significantly lower than that of the CMC groups ($P < 0.05$; Fig. 6). The absolute value of zeta potential of CMC was significantly higher than that of CMC/ACP ($P < 0.05$).

4. Discussion

Early caries and WSLs are characterised by demineralisation of the enamel surface, which is attributable to the action of acids, among which organic acids produced by bacteria are of great importance. Acidogenic bacteria on the enamel surface form plaque biofilm, which plays an important regulatory role in mineral deposition by decreasing the pH of the microenvironment, leading to demineralisation of the tooth surface [45]. Remineralisation—which meets the requirements of MID—is the desired approach to reverse this process; however, failure to inhibit the colonisation of acid-producing bacteria during treatment can result in dental plaque and calculus formation.

CMC consists of long chains harbouring carboxymethyl groups that protect calcium ions on the inner side of the ACP particles from negatively charged phosphate ions [28,46]. We found that the CMC solution was transparent without any particle deposition after sequential addition of Ca^{2+} and HPO_4^{2-}; moreover, the nanocomplexes could be stored for over a week without precipitation. Accordingly, no crystallites were observed by TEM and SAED (Fig. 1), indicating that the CMC/ACP nanocomplexes are stable.

In this study, 1% CMC/ACP had no effect on the growth and viability of *S. mutans*, *S. gordonii*, and *F. nucleatum* after 24 h (Table 1), suggesting that it does not alter the oral microbiome profile. This is important since antimicrobial agents that disrupt the balance of normal flora in the oral cavity can promote the proliferation of opportunistic pathogens [47].

Bacterial cell adherence is the first step in dental plaque formation; *S. mutans* is the predominant cariogenic bacterial species that attaches to the salivary membrane on the enamel surface [48]. Our results demonstrate that CMC/ACP reduced early adherence (Fig. 2) and 24-h biofilm formation (Fig. 3) of *S. mutans* and *S. gordonii* on saliva-coated enamel blocks, indicating that it can prevent acidification of the local environment and consequently, secondary colonisation by *F. nucleatum* and late colonisation by periodontal pathogens such as *Porphyromonas gingivalis* and *Treponema denticola* [41,49]. Indeed, we found that CMC/ACP inhibited the adherence of *F. nucleatum* to pre-formed streptococcal biofilm (Fig. 4), confirming our hypothesis that CMC/ACP nanocomplexes can inhibit the adherence of and biofilm formation by cariogenic bacterial species on enamel and the co-adhesion of *F. nucleatum*. CMC/ACP and CMC had comparable effects on *S. mutans*, *S. gordonii*, and *F. nucleatum*, suggesting that the anti-cariogenic activity of CMC was not affected when it was used as a stabilizer of the ACP cluster.

Surface charge is an important determinant of the binding between bacteria and a substrate, which affects biofilm formation [50]. Bacteria typically have a negatively charged surface [44,51]. Cytochrome c is a low molecular mass protein with a positive charge and a redox-active haem group [52,53]. In this study, we used cytochrome c and zeta potential measurements to estimate the relative surface charge of bacteria. CMC/ACP decreased the binding of cytochrome c to bacterial cells, which may be explained by the large number of cationised amino groups in CMC/ACP that may have fully or partially neutralised the negative charge on the cell surface. Surface charge is an important parameter for flocculation, which affects bacterial adhesion [54,55]. In this study, the zeta potential of *S. mutans* suspension had a negative value (−38.2 mV), which is consistent with previous reports [44,51]. The value decreased significantly after the cells were incubated with CMC or CMC/ACP for 1 h, possibly due to surface charge neutralisation and consequent depolarisation of the bacterial cell membrane. The decrease in zeta potential also suggests that the stability of the suspension was decreased by the addition of CMC or CMC/ACP, which can lead to enhanced flocculation of particles in the mixed solution [56] as well as weakened adherence among bacteria and between bacteria and the substrate surface.

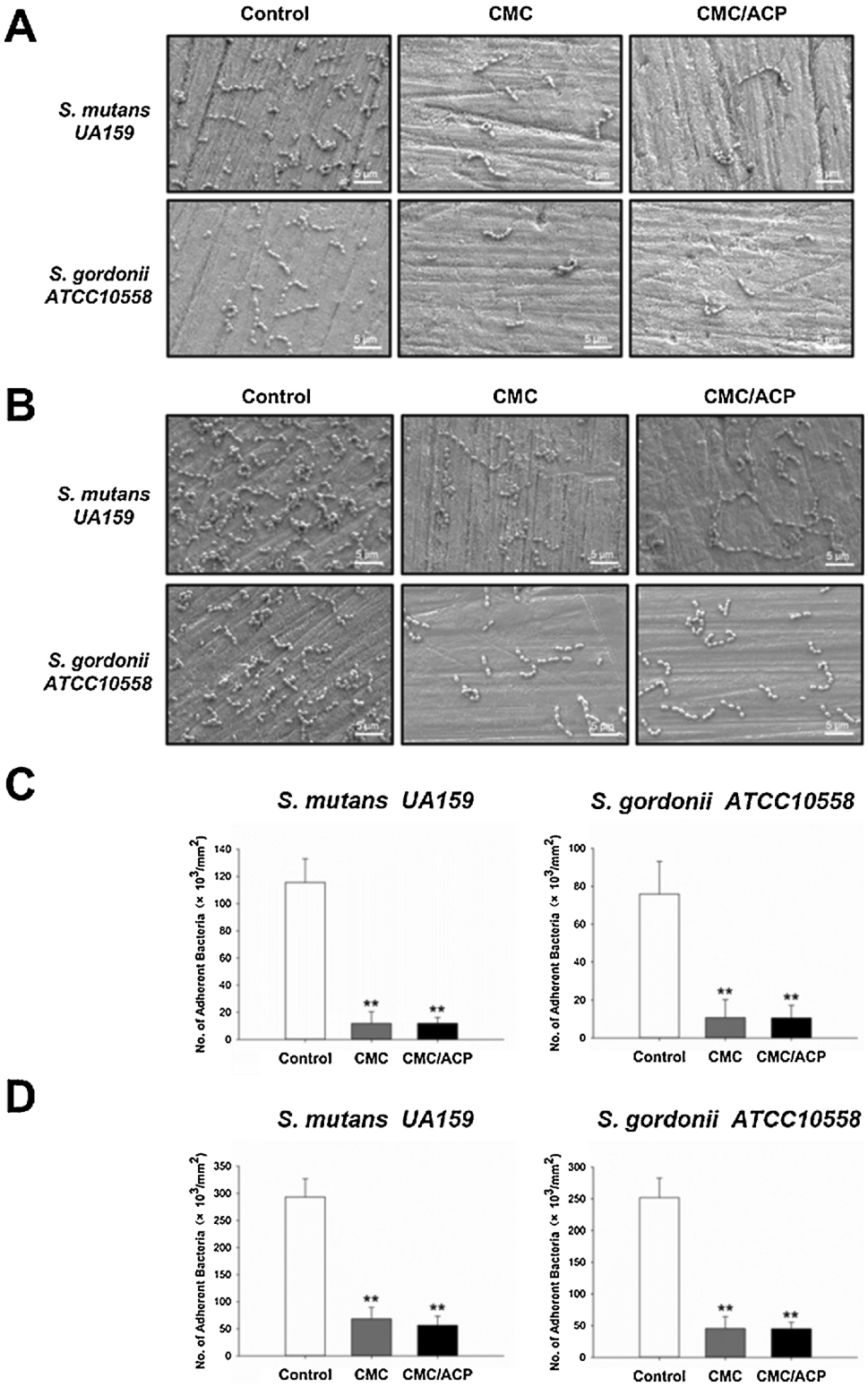

Fig. 2. Effect of CMC/ACP on *S. mutans* and *S. gordonii* adherence to saliva-coated enamel blocks. The image of SEM showed the adherence of *S. mutans* and *S. gordonii* on enamel blocks (3000-fold), (A) one-hour incubation; (B) five-hour incubation. The number of bacteria in 1 mm^2 was calculated, and the representative data are shown: (C) one-hour incubation; (D) five-hour incubation. The experiments were performed three times in triplicate. **P < 0.01 compared with the control value (absence of CMC/ACP or CMC).

In summary, our results indicated that the inhibitory effects of CMC/ACP on bacterial cell adherence and biofilm formation may be relevant to the large number of cationised amino groups in CMC/ACP, which could fully or partially neutralise the negative charge on the cell surface due to electrostatic attraction; moreover, flocculation was enhanced, which weakened the adhesion between bacteria. In addition, the flocculation could also be enhanced by the high molecular weight of CMC/ACP due to the bridging mechanism, which further affected the bacterial cell adherence [57]. However, the detailed mechanism remains to be determined.

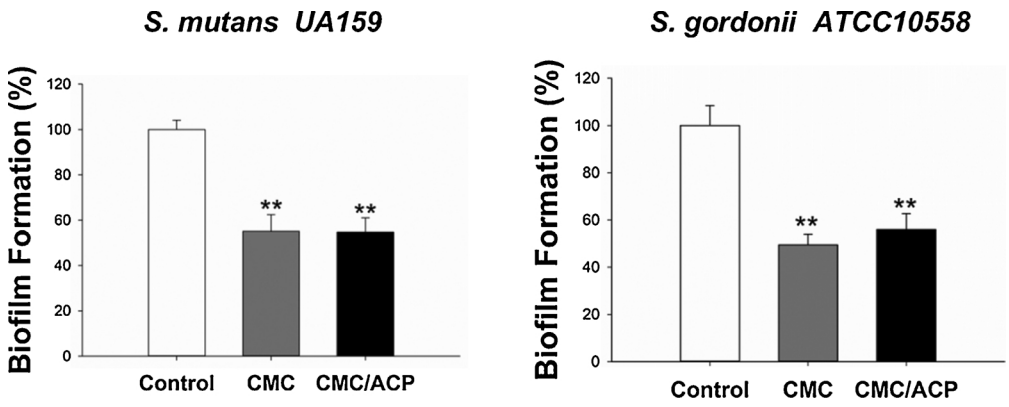

Fig. 3. Effect of CMC/ACP on *S. mutans* and *S. gordonii* biofilm formation on saliva-coated enamel block. The percent biofilm formation of *S. mutans* and *S. gordonii* are shown (control: 100%). The experiments were performed three times in triplicate. **P < 0.01 compared with the control value (absence of CMC/ACP or CMC).

5. Conclusion

The results of this study demonstrate that CMC/ACP nanocomplexes were effective in blocking the adherence of and biofilm formation by cariogenic bacteria. These effects were exerted at least in part through alteration of the surface charge of bacteria and consequent enhancement of flocculation. Given its ability to promote remineralisation and inhibit biofilm formation, CMC/ACP has potential applications in clinical dentistry for the prevention and treatment of early caries and WSLs.

Declaration of interests

There are no known conflicts of interest associated with this publication and there has been no significant financial support for this work that could have influenced its outcome.

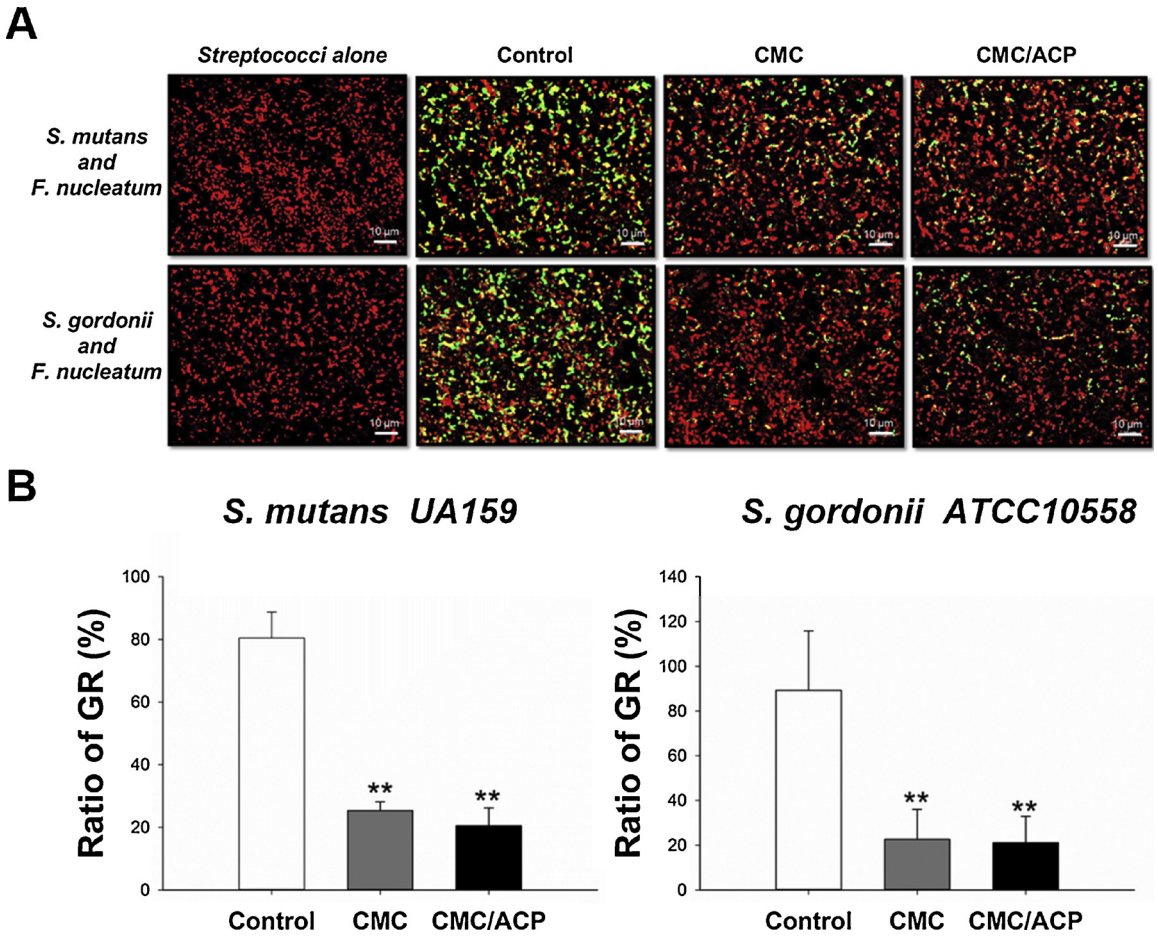

Fig. 4. Effect of CMC/ACP on *F. nucleatum* attachment to pre-formed streptococcal biofilm on saliva-coated hydroxyapatite disc. The image of CLSM (A) showed CFSE-labelled *F. nucleatum* (green) bound to pre-formed *S. mutans* and *S. gordonii* biofilm (red). The ratio of GR was determined, and the representative data was showed (B). The experiments were performed three times in triplicate. **P < 0.01 compared with the control value (absence of CMC/ACP or CMC) (For interpretation of the references to colour in this figure legend, the reader is referred to the web version of this article).

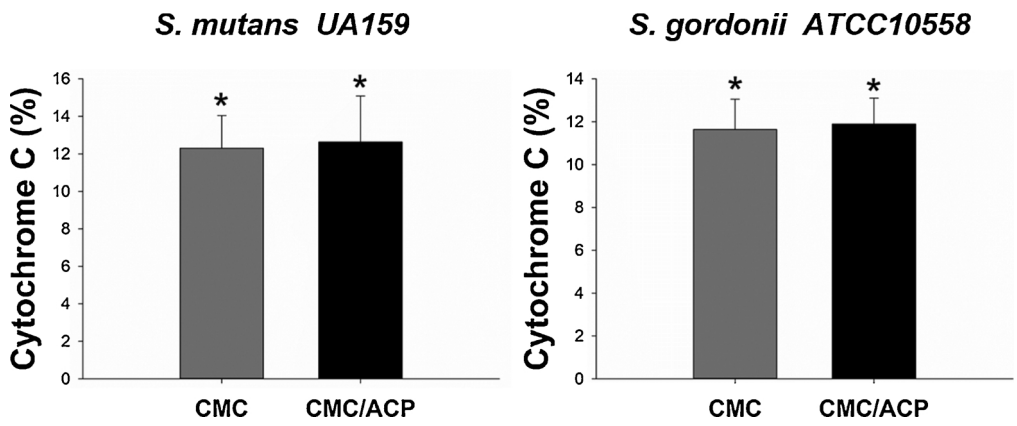

Fig. 5. Effect of CMC/ACP on cell surface charge. The percent change in cytochrome c bound to the cells was calculated, and the representative data are shown. The experiments were performed three times in triplicate. *P < 0.05 compared with the control value (absence of CMC/ACP or CMC).

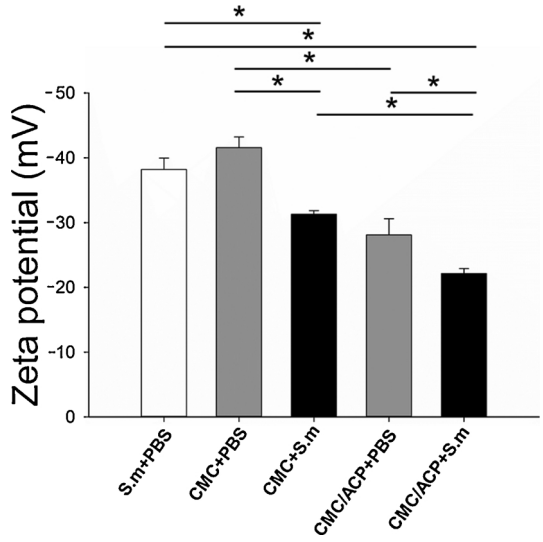

Fig. 6. The average zeta potential of CMC, CMC/ACP, untreated *S. mutans* and the mixture that mixed *S. mutans* suspension with CMC or CMC/ACP for 1 h. The experiments were performed three times in triplicate, *P < 0.05.

Acknowledgements

This study was supported by the National Natural Science Foundation of China (no. 81571016 and no. 31870947), National Natural Science Foundation of Tianjin (no. 13JCYBJC41300), and Research Fund of Stomatology School in Tianjin Medical University of China (no. 2015YKYQ01).

References

[1] Y. Liu, Y. Xu, Q. Song, F. Wang, L. Sun, L. Liu, X. Yang, J. Yi, Y. Bao, H. Ma, H. Huang, C. Yu, Y. Huang, Y. Wu, Y. Li, Anti-biofilm activities from *Bergenia crassifolia* leaves against *Streptococcus mutans*, Front. Microbiol. 8 (2017) 1738, https://doi.org/10.3389/fmicb.2017.01738.

[2] M. Khoroushi, M. Kachuie, Prevention and treatment of white spot lesions in orthodontic patients, Contemp. Clin. Dent. 8 (2017) 11–19, https://doi.org/10.4103/ccd.ccd_216_17.

[3] K.C. Julien, P.H. Buschang, P.M. Campbell, Prevalence of white spot lesion formation during orthodontic treatment, Angle Orthod. 83 (2013) 641–647, https://doi.org/10.2319/071712-584.1.

[4] A.B. Paula, A.R. Fernandes, A.S. Coelho, C.M. Marto, M.M. Ferreira, F. Caramelo, V.F. Do, E. Carrilho, Therapies for white spot lesions – a systematic review, J. Evid. Dent. Pract. 17 (2017) 23–38, https://doi.org/10.1016/j.jebdp.2016.10.003.

[5] Y. Ma, N. Zhang, M.D. Weir, Y. Bai, H.H.K. Xu, Novel multifunctional dental cement to prevent enamel demineralization near orthodontic brackets, J. Dent. 64 (2017) 58–67, https://doi.org/10.1016/j.jdent.2017.06.004.

[6] J.D. Featherstone, A. Lussi, Understanding the chemistry of dental erosion, Monogr. Oral Sci. 20 (2006) 66–76, https://doi.org/10.1159/000093351.

[7] R.P. Shellis, M.E. Barbour, A. Jesani, A. Lussi, Effects of buffering properties and undissociated acid concentration on dissolution of dental enamel in relation to pH and acid type, Caries Res. 47 (2013) 601–611, https://doi.org/10.1159/000351641.

[8] C. González-Cabezas, The chemistry of caries: remineralization and demineralization events with direct clinical relevance, Dent. Clin. North Am. 54 (2010) 469–478, https://doi.org/10.1016/j.cden.2010.03.004.

[9] K.R. Gujjar, Minimally invasive dentistry – a review, Int. J. Clin. Prev. Dent. 9 (2013) 109–120.

[10] A.K. Burwell, T. Thulamata, L.B. Gower, S. Habelitz, M. Kurylo, S.P. Ho, Y.C. Chien, J. Cheng, N.F. Cheng, S.A. Gansky, Functional remineralization of dentin lesions using polymer-induced liquid-precursor process, PLoS One 7 (2012) e38852, , https://doi.org/10.1371/journal.pone.0038852.

[11] N.J. Cochrane, F. Cai, N.L. Huq, M.F. Burrow, E.C. Reynolds, New approaches to enhanced remineralization of tooth enamel, J. Dent. Res. 89 (2010) 1187–1197, https://doi.org/10.1177/0022034510376046.

[12] S. Raphael, A. Blinkhorn, Is there a place for Tooth Mousse in the prevention and treatment of early dental caries? A systematic review, BMC Oral Health 15 (2015) 113, https://doi.org/10.1186/s12903-015-0095-6.

[13] O.B. Al-Batayneh, R.A. Jbarat, S.N. Al-Khateeb, Effect of application sequence of fluoride and CPP-ACP on remineralization of white spot lesions in primary teeth: an in-vitro study, Arch. Oral Biol. 83 (2017) 236–240, https://doi.org/10.1016/j.archoralbio.2017.08.003.

[14] J.P. Bernimoulin, Recent concepts in plaque formation, J. Clin. Periodontol. 30 (2010) 7–9.

[15] D.J. White, Dental calculus: recent insights into occurrence, formation, prevention, removal and oral health effects of supragingival and subgingival deposits, Eur. J. Oral Sci. 105 (2010) 508–522.

[16] R.J. Palmer Jr., S.M. Gordon, J.O. Cisar, P.E. Kolenbrander, Coaggregation-mediated interactions of streptococci and actinomyces detected in initial human dental plaque, J. Bacteriol. 185 (2003) 3400–3409, https://doi.org/10.1128/JB.185.11.3400-3409.2003.

[17] P.E. Kolenbrander, R.J. Palmer Jr., S. Periasamy, N.S. Jakubovics, Oral multispecies biofilm development and the key role of cell-cell distance, Nat. Rev. Microbiol. 8 (2010) 471–480, https://doi.org/10.1038/nrmicro2381.

[18] B.J. Keijser, E. Zaura, S.M. Huse, J.M. van der Vossen, F.H. Schuren, R.C. Montijn, J.M. ten Cate, W. Crielaard, Pyrosequencing analysis of the oral microflora of healthy adults, J. Dent. Res. 87 (2008) 1016–1020, https://doi.org/10.1177/154405910808701104.

[19] E.M. Bik, C.D. Long, G.C. Armitage, P. Loomer, J. Emerson, E.F. Mongodin, K.E. Nelson, S.R. Gill, C.M. Fraserliggett, D.A. Relman, Bacterial diversity in the oral cavity of 10 healthy individuals, ISME J. 4 (2010) 962–974, https://doi.org/10.1038/ismej.2010.30.

[20] R.J. Palmer Jr., N. Shah, A. Valm, B. Paster, F. Dewhirst, T. Inui, J.O. Cisar, Interbacterial adhesion networks within early oral biofilms of single human hosts, Appl. Environ. Microbiol. 83 (2017), https://doi.org/10.1128/AEM.00407-17 pii: e00407-17.

[21] R. Nomura, R. Yoneyama, S. Naka, M. Otsugu, Y. Ogaya, R. Hatakeyama, Y. Morita, J. Maruo, M. Matsumoto-Nakano, O. Yamada, K. Nakano, The *in vivo* inhibition of oral biofilm accumulation and *Streptococcus mutans* by ceramic water, Caries Res. 51 (2017) 58–67, https://doi.org/10.1159/000452343.

[22] G. Kaur, S. Rajesh, S.A. Princy, Plausible drug targets in the *Streptococcus mutans* quorum sensing pathways to combat dental biofilms and associated risks, Indian J. Microbiol. 55 (2015) 349–356, https://doi.org/10.1007/s12088-015-0534-8.

[23] N.S. Jakubovics, J.C. Robinson, D.S. Samarian, E. Kolderman, S.A. Yassin, D. Bettampadi, M. Bashton, A.H. Rickard, Critical roles of arginine in growth and biofilm development by *Streptococcus gordonii*, Mol. Microbiol. 97 (2015) 281–300.

[24] A.H. Nobbs, H.F. Jenkinson, N.S. Jakubovics, Stick to your gums: mechanisms of oral microbial adherence, J. Dent. Res. 90 (2011) 1271–1278.

[25] C.W. Kaplan, R. Lux, S.K. Haake, W. Shi, The *Fusobacterium nucleatum* outer membrane protein RadD is an arginine-inhibitable adhesin required for inter-species adherence and the structured architecture of multi-species biofilm, Mol.

Microbiol. 71 (2009) 35–47.
[26] B. Biyikoğlu, A. Ricker, P.I. Diaz, Strain-specific colonization patterns and serum modulation of multi-species oral biofilm development, Anaerobe 18 (2012) 459–470, https://doi.org/10.1016/j.anaerobe.2012.06.003.
[27] A. Sakanaka, M. Kuboniwa, H. Takeuchi, E. Hashino, A. Amano, Arginine-ornithine antiporter ArcD controls arginine metabolism and interspecies biofilm development of *Streptococcus gordonii*, J. Biol. Chem. 290 (2015) 21185–21198, https://doi.org/10.1074/jbc.M115.644401.
[28] Z. Xiao, K. Que, H. Wang, R. An, Z. Chen, Z. Qiu, M. Lin, J. Song, J. Yang, D. Lu, M. Shen, B. Guan, Y. Wang, X. Deng, X. Yang, Q. Cai, J. Deng, L. Ma, X. Zhang, X. Zhang, Rapid biomimetic remineralization of the demineralized enamel surface using nano-particles of amorphous calcium phosphate guided by chimaeric peptides, Dent. Mater. 33 (2017) 1217–1228, https://doi.org/10.1016/j.dental.2017.07.015.
[29] Z. Chen, S. Cao, H. Wang, Y. Li, A. Kishen, X. Deng, X. Yang, Y. Wang, C. Cong, H. Wang, Biomimetic remineralization of demineralized dentine using scaffold of CMC/ACP nanocomplexes in an *in vitro* tooth model of deep caries, PLoS One 10 (2015) e0116553, , https://doi.org/10.1371/journal.pone.0116553.
[30] Y. Tan, F. Han, S. Ma, W. Yu, Carboxymethyl chitosan prevents formation of broad-spectrum biofilm, Carbohydr. Polym. 84 (2011) 1365–1370, https://doi.org/10.1016/j.carbpol.2011.01.036.
[31] Y. Tan, S. Ma, C. Liu, W. Yu, F. Han, Enhancing the stability and antibiofilm activity of DspB by immobilization on carboxymethyl chitosan nanoparticles, Microbiol. Res. 178 (2015) 35–41, https://doi.org/10.1016/j.micres.2015.06.001.
[32] L. Cheng, M.D. Weir, H.H. Xu, J.M. Antonucci, A.M. Kraigsley, N.J. Lin, S. Lin-Gibson, X. Zhou, Antibacterial amorphous calcium phosphate nanocomposites with a quaternary ammonium dimethacrylate and silver nanoparticles, Dent. Mater. 28 (2012) 561–572, https://doi.org/10.1016/j.dental.2012.01.005.
[33] Y. Wang, N. Van Manh, H. Wang, X. Zhong, X. Zhang, C. Li, Synergistic intrafibrillar/extrafibrillar mineralization of collagen scaffolds based on a biomimetic strategy to promote the regeneration of bone defects, Int. J. Nanomed. 11 (2016) 2053–2067.
[34] S.J. Ahn, S.J. Ahn, Z.T. Wen, L.J. Brady, R.A. Burne, Characteristics of biofilm formation by *Streptococcus mutans* in the presence of saliva, Infect. Immun. 76 (2008) 4259–4268, https://doi.org/10.1128/IAI.00422-08.
[35] F. Wahid, H.S. Wang, Y.S. Lu, C. Zhong, L.Q. Chu, Preparation, characterization and antibacterial applications of carboxymethyl chitosan/CuO nanocomposite hydrogels, Int. J. Biol. Macromol. 101 (2017) 690–695, https://doi.org/10.1016/j.ijbiomac.2017.03.132.
[36] S.C. Fernandes, P. Sadocco, A. Alonsovarona, T. Palomares, A. Eceiza, A.J. Silvestre, I. Mondragon, C.S. Freire, Bioinspired antimicrobial and biocompatible bacterial cellulose membranes obtained by surface functionalization with aminoalkyl groups, ACS Appl. Mater. Interfaces 5 (2013) 3290–3297, https://doi.org/10.1021/am400338n.
[37] K. Hirota, H. Yumoto, K. Miyamoto, N. Yamamoto, K. Murakami, Y. Hoshino, T. Matsuo, Y. Miyake, MPC-polymer reduces adherence and biofilm formation by oral bacteria, J. Dent. Res. 90 (2011) 900–905, https://doi.org/10.1177/0022034511402996.
[38] Y.J. Jang, Y.J. Choi, S.H. Lee, H.K. Jun, B.K. Choi, Autoinducer 2 of *Fusobacterium nucleatum* as a target molecule to inhibit biofilm formation of periodontopathogens, Arch. Oral Biol. 58 (2013) 17–27, https://doi.org/10.1016/j.archoralbio.2012.04.016.
[39] M. Kuboniwa, E.L. Hendrickson, Q. Xia, T. Wang, H. Xie, M. Hackett, R.J. Lamont, Proteomics of *Porphyromonas gingivalis* within a model oral microbial community, BMC Microbiol. 9 (2009) 98, https://doi.org/10.1186/1471-2180-9-98.
[40] P. Kalia, A. Jain, R. Radha Krishnan, D.R. Demuth, J.M. Steinbach-Rankins, Peptide-modified nanoparticles inhibit formation of *Porphyromonas gingivalis* biofilms with *Streptococcus gordonii*, Int. J. Nanomed. 12 (2017) 4553–4562, https://doi.org/10.2147/IJN.S139178.
[41] Y.J. Jang, J. Sim, H.K. Jun, B.K. Choi, Differential effect of autoinducer 2 of *Fusobacterium nucleatum* on oral streptococci, Arch. Oral Biol. 58 (2013) 1594–1602, https://doi.org/10.1016/j.archoralbio.2013.08.006.
[42] A. Jastrzebska, E. Karwowska, A. Olszyna, Influence of the *Staphylococcus aureus* bacteria cells on the zeta potential of graphene oxide modified with alumina nanoparticles in electrolyte and drinking water environment, in: A. Oral, Z. Bahsi Oral, M. Ozer (Eds.), 2nd International Congress on Energy Efficiency and Energy Related Materials (ENEFM2014), Springer Proceedings in Energy (2015) 245–250.
[43] F. Tokumasu, G.R. Ostera, C. Amaratunga, R.M. Fairhurst, Modifications in erythrocyte membrane zeta potential by *Plasmodium falciparum* infection, Exp. Parasitol. 131 (2012) 245–251, https://doi.org/10.1016/j.exppara.2012.03.005.
[44] S. Halder, K.K. Yadav, R. Sarkar, S. Mukherjee, P. Saha, S. Haldar, S. Karmakar, T. Sen, Alteration of zeta potential and membrane permeability in bacteria: a study with cationic agents, Springerplus 4 (2015) 672, https://doi.org/10.1186/s40064-015-1476-7.
[45] M. Ohta, H. Gotouda, T. Ito, N.S. Kuwahara, T. Kurita Ochiai, C. Taguchi, I. Nasu, M. Shimosaka, Evaluation of the proportion of cariogenic bacteria associated with dental caries, Epidemiol. Open Access 7 (2017) 5, https://doi.org/10.4172/2161-1165.1000327.
[46] P.J. Smeets, K.R. Cho, R.G. Kempen, N.A. Sommerdijk, J.J. De Yoreo, Calcium carbonate nucleation driven by ion binding in a biomimetic matrix revealed by in situ electron microscopy, Nat. Mater. 14 (2015) 394–399, https://doi.org/10.1038/nmat4193.
[47] S.U. Maheswari, J. Raja, A. Kumar, R.G. Seelan, Caries management by risk assessment: a review on current strategies for caries prevention and management, J. Pharm. Bioallied Sci. 7 (2015) 320–324, https://doi.org/10.4103/0975-7406.163436.
[48] M.I. Klein, G. Hwang, P.H. Santos, O.H. Campanella, H. Koo, *Streptococcus mutans*-derived extracellular matrix in cariogenic oral biofilms, Front. Cell. Infect. Microbiol. 5 (2015) 10, https://doi.org/10.3389/fcimb.2015.00010.
[49] S. Periasamy, P.E. Kolenbrander, Mutualistic biofilm communities develop with *Porphyromonas gingivalis* and initial, early, and late colonizers of enamel, J. Bacteriol. 91 (2009) 6804–6811, https://doi.org/10.1128/JB.01006-09.
[50] F. Song, H. Koo, D. Ren, Effects of material properties on bacterial adhesion and biofilm formation, J. Dent. Res. 94 (2015) 1027–1034, https://doi.org/10.1177/0022034515587690.
[51] J. Cieśla, A. Bieganowski, M. Janczarek, T. Urbanik-Sypniewska, Determination of the electrokinetic potential of *Rhizobium leguminosarum* bv trifolii Rt24.2 using laser Doppler velocimetry – a methodological study, J. Microbiol. Methods 85 (2011) 199–205, https://doi.org/10.1016/j.mimet.2011.03.004.
[52] I. Gomes, M.J. Feio, N.C. Santos, P. Eaton, A.P. Serro, B. Saramago, E. Pereira, R. Franco, Controlled adsorption of cytochrome c to nanostructured gold surfaces, J. Nanopart. Res. 14 (2012) 1–12, https://doi.org/10.1007/s11051-012-1321-7.
[53] S. Imabayashi, T. Mita, T. Kakiuchi, Effect of the electrostatic interaction on the redox reaction of positively charged cytochrome c adsorbed on the negatively charged surfaces of acid-terminated alkanethiol monolayers on a Au(111) electrode, Langmuir 21 (2005) 1470–1474, https://doi.org/10.1021/la047992x.
[54] A. Schmitt, A. Fernández-Barbero, M. Cabrerizo-Vílchez, R. Hidalgo-Álvarez, Experimental evidence regarding the influence of surface charge on the bridging flocculation mechanism, in: T. Palberg, M. Ballauff (Eds.), Optical Methods and Physics of Colloidal Dispersions. Progress in Colloid & Polymer Science, vol. 104, Steinkopff, Dresden, 1997pp. 144–147.
[55] K.J. Verstrepen, F.M. Klis, Flocculation, adhesion and biofilm formation in yeasts, Mol. Microbiol. 60 (2006) 5–15, https://doi.org/10.1111/j.1365-2958.2006.05072.x.
[56] E. Ofir, Y. Oren, A. Adin, Electroflocculation: the effect of zeta-potential on particle size, Desalination 204 (2007) 33–38, https://doi.org/10.1016/j.desal.2006.03.533.
[57] S.P. Strand, K.M. Vårum, K. Østgaard, Interactions between chitosans and bacterial suspensions: adsorption and flocculation, Colloids Surf. B Biointerfaces 27 (2003) 71–81.